Available online at www.sciencedirect.com
SCIENCE DIRECT®
ELSEVIER
Geomorphology 58 (2004) 339–355
GEOMORPHOLOGY
www.elsevier.com/locate/geomorph

Morphology, mineralogy and magnetic susceptibility of epikarst-Terra Rossa developed in late Quaternary aeolianite deposits of southeastern Saurashtra, India

Aniruddha S. Khadkikar[a,*], Nathani Basavaiah[b]

[a] *Geology and Palaeontology Group, Agharkar Research Institute, G.G. Agarkar Road, Pune 411004, India*
[b] *Indian Institute of Geomagnetism, Colaba, Mumbai, India*

Received 28 October 2002; received in revised form 8 July 2003; accepted 18 July 2003

Abstract

The nature and development of epikarst and soil development in aeolianites under a monsoonal climatic regime has not yet been described. Late Quaternary aeolianites of the southeastern coast of Saurashtra in western India show a wide array of epikarst and red-soil formation, and serve to typify the character of aeolianite weathering under a monsoonal climate. Three varieties of epikarst are identified that represent down-profile increase in groundwater flow. Five types of Terra Rossae represent a transition from the karstified limestone to soil development. Terra Rossae differ in the content of residual aeolianite and show both simple and complex profiles. The latter at places shows ped development. The results show that an ontogenetic (growth) sequence exists from incipient epikarst to complex palaeosols. This ontogenetic sequence represents an incremental increase in the groundwater budget of the region in response to changing intensification of the Indian monsoon rainfall. Magnetic properties of the Terra Rossae formed under a monsoonal climate are described for the first time. The magnetic susceptibility together with its frequency-dependent and anhysteretic remanent magnetization (ARM) represents both the concentration of single domain and ultrafine superparamagnetic (SP) magnetite. The formation of single domain and superparamagnetic magnetite and hematite are linked genetically to weathering of the aeolianite that leads to the formation of Terra Rossa.

Keywords: Epikarst; Terra Rossa; Monsoon; India; Aeolianite; Carbonate; Diagenesis; Magnetic susceptibility

1. Introduction

The nature and development of epikarst and soil development in aeolianites under a monsoonal climatic regime has not yet been described. Karst features that include only different varieties of solution pipes are not reported in the classic Bahamas and Bermuda (Kindler and Hearty, 1997; Vacher and Rowe, 1997) outcrops, although red beds are present (Herwitz et al., 1996). Karst phenomena in aeolianites of Bahamas, Bermuda and Australia usually consist of caves, dolines, etc. (Mylorie and Carew, 1995). Red soils are commonly developed on limestones under a Mediterranean type of climate (Yaalon, 1997) and are also reported from tropical regions (Bronger and Bruhn-

* Corresponding author.
E-mail address: askhadkikar@yahoo.com (A.S. Khadkikar).

0169-555X/$ - see front matter © 2003 Elsevier B.V. All rights reserved.
doi:10.1016/j.geomorph.2003.07.001

Lobin, 1997). These have been termed Terra Rossa and appear to be typical of Mediterranean regions, which experience rainfall during the winter months. Terra Rossa soils are currently understood to have formed by leaching and residual accumulation of limestone (Bronger and Bruhn-Lobin, 1997) although alternative hypotheses that propose Saharan dust addition exist (Herwitz et al., 1996). Late Quaternary aeolianites occur along the coast of Saurashtra in western India. This region is governed by the Indian Summer Monsoon, which is spread over 3 months from mid-June to August. The aeolianites show a wide array of epikarst and red-soil formation, and serve to typify the character of aeolianite weathering under a monsoonal climate. The purpose of the paper is to describe the field characteristics of epikarst and Terra Rossa in the aeolianites. Additionally, studies were also undertaken to characterize the bulk mineralogy using X-ray diffractometry (XRD) and Fourier transform infrared (FTIR) spectroscopy and the magnetic susceptibility of the Terra Rossa palaeosols.

2. Area of study

Along the southern coast of Saurashtra, a suite of carbonate rocks regionally known as the Miliolite crop out. These outcrops occur as coast-parallel ridges and cliffs. The latter are up to 40 m in height and have formed through wave erosion. The Miliolites are white to buff in colour and show large-scale cross bedding. These deposits generally become more impure along a west to east transect, i.e., the Miliolites towards the Porbandar–Dwarka region are more carbonate rich. The sediments that are essentially pelletoid, and oolitic bioclastic calc-arenites (Merh, 1980) were first named ‘Miliolite’ by Carter (1849) owing to the predominance of bioclasts belonging to the fora-

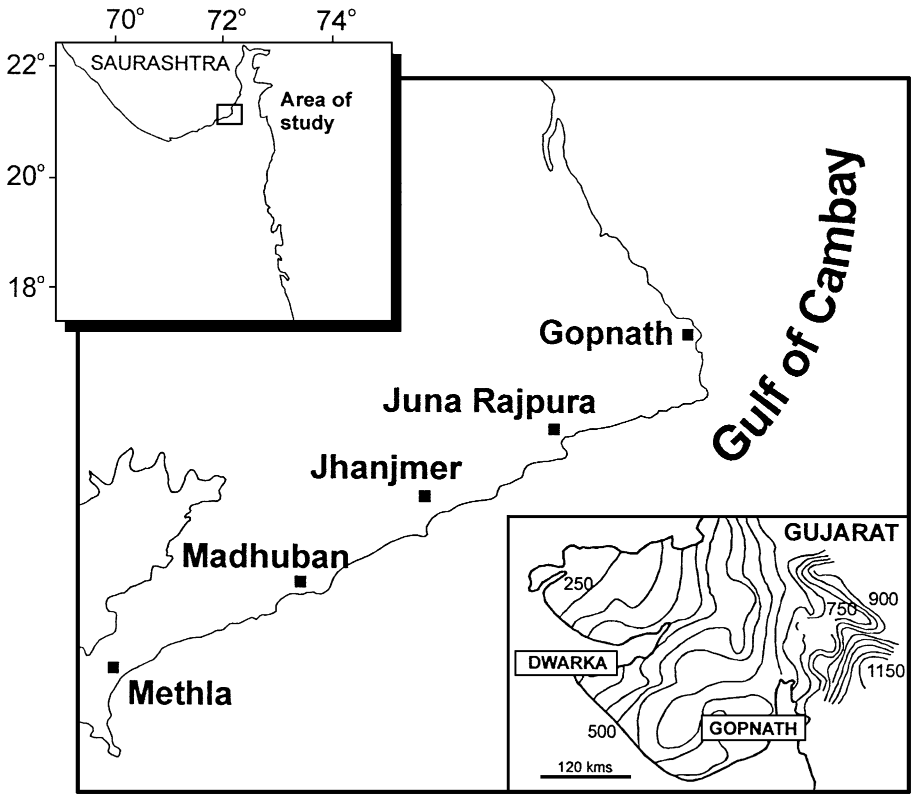

Fig. 1. Location map of the aeolianite outcrops studied in southeastern Saurashtra. The Miliolite was mapped along the coast using photopanels between A and B and an event stratigraphy erected (see Fig. 8). Inset shows the modern rainfall distributions in the region.

miniferal genus *Miliolina*. The current study is based on outcrops located in southeastern Saurashtra between Gopnath and Methla (Fig. 1).

Saurashtra is influenced by the vagaries of the Southwest Indian Monsoon (SWIM), which normally onsets around the 15th of June every year and extends its influence for a period varying between 2 and 3 months (Das, 1995). The SWIM is propelled by temperature contrasts between land and ocean masses. Such differences come about due to the greater heat capacity of the ocean relative to land. During the summer season, high solar radiation induces heating over the Tibetan plateau and northern India. This generates a pressure gradient; the warmer Asian continent becomes an area of low pressure while the Indian Ocean represents a high-pressure region (Madagascar high). This pressure gradient leads to low level southwesterly summer monsoon winds, i.e., the Southwest Indian Monsoon. In the winter months, wind in the opposing direction is generated, whose genesis again lies in the differential heat capacities of land and ocean masses. These winds flow from northeastern India over much of Gujarat and Rajasthan towards the Indian Ocean. These monsoon winds, however, do not yield rain over the state of Gujarat. The southeastern coast of Saurashtra shows a progressive decrease in rainfall from east to west. While regions around Gopnath and Gadhula experience mean annual rainfalls around 700–500 mm, regions towards the west near Dwarka are typically semi-arid to arid receiving mean annual rainfalls as low as 300 mm (Fig. 1).

3. Karst

The German word ‘karst’ is derived from the Slav word Krś meaning crag or stone and now refers to the geomorphology of limestone terrains. Jennings (1985) defined ‘karst’ to signify terrains with distinctive characteristics of relief and drainage arising primarily from a higher degree of rock solubility in natural waters than is found elsewhere. In the present study, the word ‘karst’ is used to refer to dissolution features found pervasively developed in aeolianites. The ‘karst’ is essentially variants of solution pipes that are vertically oriented, sometimes interconnected to form a honeycomb network or appear as an irregular surface dominated by cavities and channels. Most of the variants of karst are ‘epikarst’, i.e., solution features that have developed near the surface within depths extending to a few meters only. Based on surface morphology of the karst, various types designated as “Type 1, 2 or 3” karst are documented. The criteria chosen for the differentiation are:

- diameter/area of voids as seen in planform,
- vertical connectivity
- density of voids/thickness of encompassing walls and
- sharpness of the walls.

3.1. Type 1 karst

This type of karst consists of cavities that are in the centimeter scale and commonly within 5 cm in diameter (Fig. 2a). The planform of the cavities is highly irregular. The density of the cavities is also very high. The cavities are separated by thin walls that again are very irregular in shape. This causes the mass to be dominated more by cavities than by the limestone itself. Such irregularity lends a chaotic structure to the limestone in the field. The orientation of the cavities is random and is mostly as interconnected networks. The thickness of such a karst type rarely exceeds 0.5 m. This type of karst occurs by itself or is part of a complex karst profile commonly forming the upper zone. Some cavities also coalesce to form larger cavities in some parts. The walls also contain concave up depressions. Some distinct vertical cavities are also observed within the same exposure.

3.2. Type 2 karst

Type 2 karst is the most common variety, and it is typified by cavities of near circular planform shape. These cavities are between 3 and 7 cm in maximum diameter (Fig. 2b). Like the previous variety, this type of epikarst shows coalescence of cavities. The cavities extend down vertically to form pipes. Walls are thicker compared to Type 1 karst and have smoother sufaces. Lateral interconnectedness is relatively smaller, which is evident in the dominant vertical fabric. The thickness of Type 2 karst horizons is variable but is generally the largest of the karst varieties.

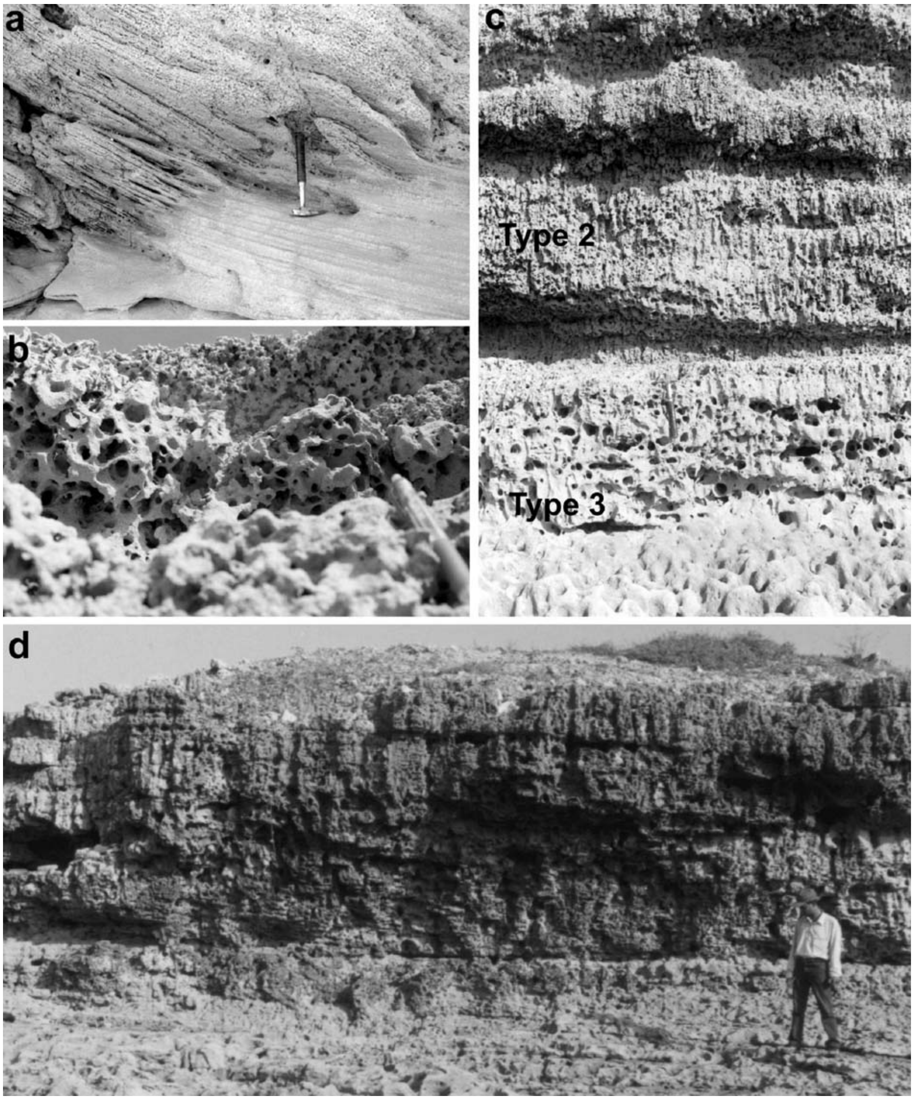

Fig. 2. (a) Type 1 karst with small interconnected cavities well developed towards the top but grades towards non-karstified aeolianite. (b) Type 2 karst with dominant vertically disposed pipes. Note coalescence of pipes. (c) Composite karst profile showing all the three varieties of karst profiles. The profiles show a progressive downprofile enlargement of the conduits. Most of the aeolianites are affected by such epikarst development as shown in (d).

3.3. Type 3 karst

This variant forms the end of a spectrum with Type 1 representing the opposing end member (Fig. 2c). The cavities are medium to large ranging in size from >5 cm to as large as 15 cm in maximum diameter. Both vertical and laterally disposed pipes are observed although the former are visibly less in number. Planform of the cavities is circular to elliptical. The walls of the solution pipes are thicker and cavity density is less than Type 2 karst. The walls are generally smooth with infrequent knobbles.

A different variety grouped in this class owing to the larger cavity dimension occurs in the modern inter-tidal zone. Here, the walls develop very sharp edges towards the upper boundary. The resulting karst has protrusions up to 10–15 cm in height (pinnacles).

3.4. Distribution of karst features

There are very few regions in the outcrop at Gopnath where some form of weathering has not affected the aeolianite. Where only cementation has occurred, primary sedimentary structures are retained; the most common being planar lamination. The first effect of karstification is the obliteration of the sedimentary structures in Type 1 karst. Type 1 karst only occurs exclusively a place where lateral variations grade from Type 1 karst to parallel laminated aeolianite.

The distribution of the other two types occurs in profile along with Type 1. In some cases where pedogenesis has progressed to the extent that soils appear, Type 1 karst may be obliterated. This leads to a reddened massive bed without cavities overlying Type 2 and sometimes Type 3 karst directly. In some sections of the outcrop at Gopnath complex superimposed profiles occur which, consist of karst Types 1, 2 and 3 stacked above each other. For example, in Fig. 3a at the top, a profile consisting of Type 1 and Type 2 karst is followed by another profile consisting of Type 1 karst overlying a very thick Type 2 karst profile (~ 1 m), which is above a Type 3 profile about 0.5 m thick.

In all profiles, the essential order of superposition is Type 1/Type 2/Type 3 (Fig. 2c,d). This becomes a very useful criterion to separate complex profiles into its individual components. The recognition of individual karst profiles becomes clear if a Type 2 karst overlies a Type 1 karst, the latter indicating the beginning of an older karst profile. The degree of lateral variability is such that within a distance of a meter a palaeosol may overlie a Type 2/Type 3 karst profile in one section and in the other overlie a Type 3 karst directly.

3.5. Interpretation

The formation of karst is stressed in the original definition (Jennings, 1985) to be due to solution processes. The primary control on the solution behaviour is the formation of weak carbonic acids by the dissolution of carbon dioxide in water to for carbonic acid. Large quantities of solution take place as water rich in carbonic acid is rapidly recharged. This weak acid interacts with the allochems in the aeolianite to dissolve and reprecipitate calcite. The new form of calcite is in the form of clotted micrite (seen in thin sections).

At the top levels of an epikarst profile, Type 1 karst is present with interconnected pores. The formation of this type of karst appears to be related to random cavity generation along primary porosities of the inter-granular type. The randomness of the channel network suggests that meteoric flow is probably diffusive in all three directions. As the waters concentrate and gain sufficient volume locally, the pores are widened to form channels and vertical gravity percolation begins. The zone where pipeflow water movement dominates is represented by the Type 2 karst. Localized solution may occur as a result of down-profile incremental saturation of pore waters with respect to calcium carbonate. Coalescence of such a vertical pipe network causes the formation of much larger pipe cavities. Successive meteoric water transported along such secondary porosities, aids in the development of larger channels and travels directly to the base of the profile. These channels are typical of Type 3 karst. Under this model, the various types of epikarst form an evolutionary sequence due to the concentration of water along channel networks and the formation of incrementally larger channels with depth from the surface.

Descriptions of such epikarst phenomena in aeolianites are few. Mylorie and Carew (1995) describe similar epikarst features in the San Salvador Island of Bahamas. Rillenkarren and runnel formation (Jennings, 1985) that are typical of limestone terrains are absent. This could be due to differences in climate conditions and/or host rock composition; the latter in the present case having a larger siliciclastic component.

3.6. Modification of karst

Karstified aeolianites are continuously modified by modern wave erosion processes. The result of this interaction between waves and karst cavities is the enlargement of the cavities and a change in the planform geometry to near circular forms. This is due to the generation of vortices in the hollows. Milling of the cavities is facilitated by small pebbles trapped in the vortices of the aeolianites. Significant enlargement is observed for toppled blocks that are oriented in such a manner that the cavities face the tides. A second effect of the inter-tidal wave action is the formation of pinnacles in the modern inter-tidal zone.

4. Terra Rossa palaeosols

4.1. Field character

The red soils are laterally extensive layers of reddened sediment that are seen to commonly interfinger with the karstified aeolianite. The thickness of the red beds varies from 3 to 7–10 cm, but is commonly between 1 and 2 m in thickness. The colour of the Terra Rossae varies from 2.5/6 YR to 5/6 YR to 10/4 R. While the upper bounding surface is sharp, the lower contact is gradational into the host aeolianite. The profiles observed in the present segment between Gopnath and Methla had some distinctive character that made each profile unique. Hence, no compartmentalization is attempted and the various types of Terra Rossa profiles are described individually below. The descriptive sequence ranges from weakly developed profiles (in terms of thickness and reddening) to strongly developed ones; from simple profiles to complex profiles. The Terra Rossae profiles are designated as Type 1, . . ., *n*. Repeated reference is made to 'residual aeolianite', which represents the weathered remains of aeolianite that existed prior to pedogenesis. The recognition of the aeolianite is clear in hand specimens and has been confirmed petrographically.

4.1.1. Type 1

The thinnest Terra Rossae is only a few centimeters thick. These are sandwiched between thicker meter scale aeolianites and have sharper upper and lower bounding surfaces. The red soils occur on bounding surfaces that dip up to 20° to near horizontal lower bounding surfaces. Texturally, the red soil is dominantly silty with some amount of clay. Colours of the red soils are dark red to brownish red.

4.1.2. Type 2

Red soils belonging to this category are observed in Jhanjmer (Fig. 3a). The upper contact is sharp and separates an overlying aeolianite. No horizonation is seen although there is a distinct loss in reddening down profile. Primary sedimentary structures are obliterated. The profile varies in thickness from 1 to 2 m. Disseminated residual aeolianite is present, which is coated with powdery calcite. The entire red layer is calcareous.

4.1.3. Type 3

This Terra Rossa is relatively strongly developed and probably represents an evolutionary stage from the previous variety. Towards the top of the profile a distinct horizon is observed, characterized by a platy structure and absence of residual carbonates. The degree of reddening is high in this horizon and so is the darkness. This is followed down profile by a horizon, which is dark reddish brown in colour and is characterized by the presence of residual carbonates. The residual carbonates are slightly elongated and are 1–4 cm in vertical dimension and give a false impression of being rhizoliths. At the base of this horizon is a third layer, which is lighter in colour (low reddening) and grades into a Type 3 epikarst (Fig. 3b).

A different type of profile is seen at Gopnath, which is interesting due to the presence of residual carbonates are in the form of spheroids. At first, they appear as calcrete nodules, which they are not. This is based on petrographic studies of the nodules that do not show typical calcrete microfabrics but on the other hand are similar to the aeolianites. This has not been observed in any other profile studied so far. The karstified spheroids are distributed randomly throughout the profile and are associated with other irregular forms of residual aeolianite, some of which is tubular in form. The base of the profile is not exposed clearly as it is within the modern inter-tidal zone. The Terra Rossa is exposed, as an exhumed outcrop so it is unclear if horizonation is present or not. The exposed estimated thickness of the horizon is about 1.3 m.

In the same region, Terra Rossae are also seen to be tightly interbedded with cross bedded aeolianites. Here, a 'graphic' contrast is seen between the white aeolianite and the bright red-coloured bed (Fig. 3c).

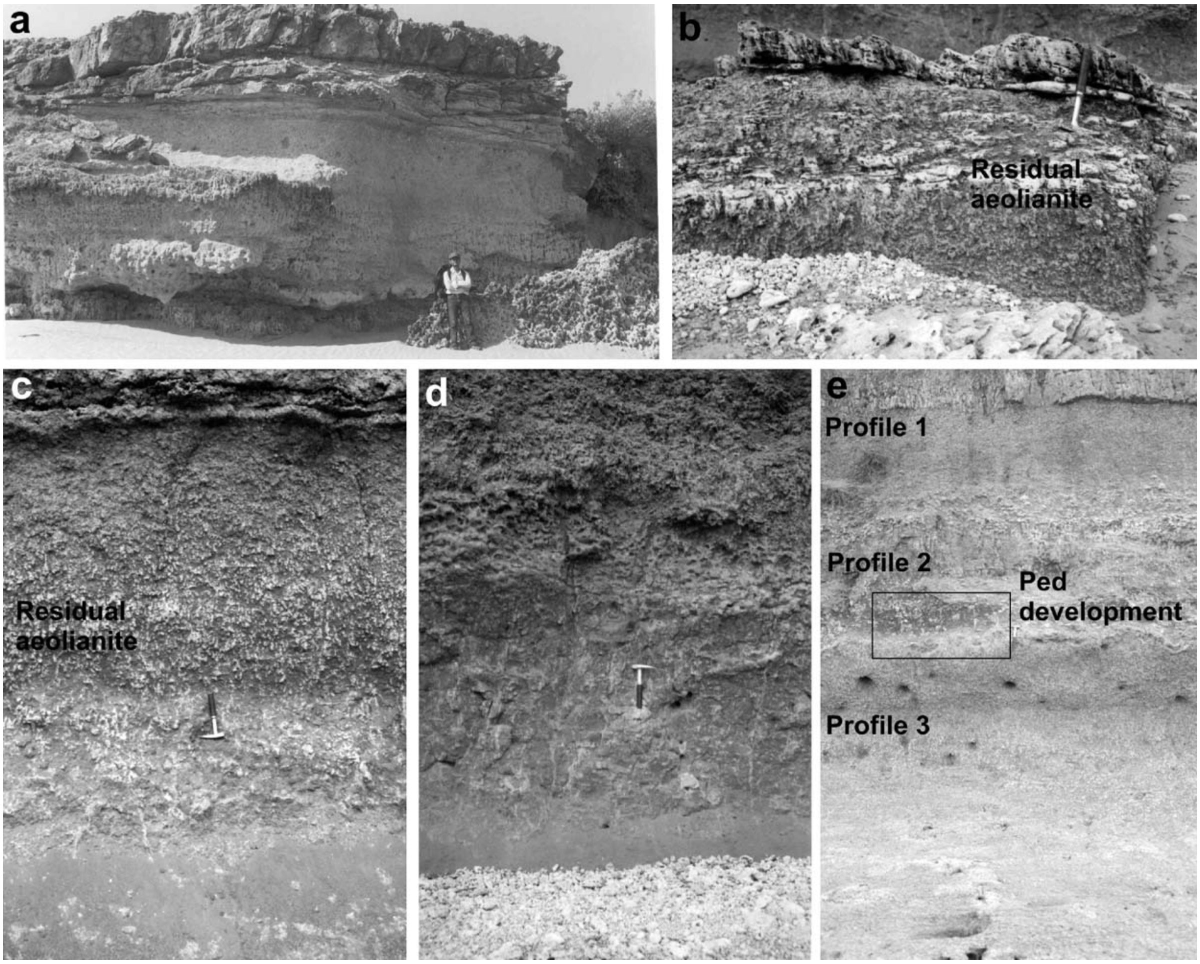

Fig. 3. (a) Lateral variations in the super-position of red bed over Type 2 and Type 3 karst. Red-soil formation of Type 2 obliterates Type 1 karst. (b, c) Terra Rossa profiles with different types of residual carbonates. In (b), note the presence of platy structure at the top and down profile loss in reddening. (c) Shows the presence of stringers of aeolianite within the Terra Rossa. (d) Terra Rossa of Type 4 showing platy structure at the top and absence of residual aeolianites within the profile. (e) Complex Terra Rossa profiles of the variety Type 5. Illustrated is the dominance of Terra Rossae and residual aeolianite throughout the profile. The rectangle draws attention to clay rich layers, which show ped development.

The aeolianite retains its primary lamination and occurs as discontinuous stringers. Neither horizonation, nor any ped development is observed in the Terra Rossa. The red-bed thickness is about 0.4–0.2 m.

4.1.4. Type 4

This profile differs from the first variant of Type 3 in the paucity of residual carbonate (Fig. 3d). The profiles are generally between 1.5 and 3 m in thickness. There is a down-profile decrease in reddening. The upper part of the profile shows platy structure development. The horizon is dark reddish brown in colour. Some primary calcium carbonate is observed in the profiles in the horizon below. This zone is weakly reddened when compared to the overlying horizon. Residual carbonates are absent although rare occurrences of very diffuse patches are seen in the lower most portions of the profile. This weakly developed horizon grades into a horizon that bears residual aeolianite scattered in a background of reddened clayey silt. This profile is laterally extensive and is by far the most common in the aeolianite at lower stratigraphic levels in most cliff sections.

4.1.5. Type 5

At Gopnath, a single section shows several superimposed red beds and weathering features throughout (Fig. 3e). At no level are aeolianites with clear internal lamination observed. Only residual carbonates, which are in the centimeter scale, and red palaeosols are stacked above each other. At the base of the section, there is a large concentration of clays within a band that is ~ 15 cm thick. This band shows blocky aggregates that are between 2 and 3 cm in height and width and are subangular. The layers show reddening and are underlain by clayey silt containing residual carbonate. For the major part of the section, residual carbonates that are in the centimeter to subcentimeter scale are distributed throughout. At the top, there appears to be a larger accumulation of clays. However, close examination was not possible due to inaccessibility of the outcrop.

4.2. Evidences of root activity

The activity of ancient roots and the presence of fauna are present in the red beds (Fig. 4). This is in the form of hollow and filled tubes. Around the hollow tubes, there usually are halos of both amorphous iron oxide, which is bright red in colour, and also, at times, the presence of powdery carbonate (Fig 4b). Filled tubes similar to phreatophytic rhizoliths are observed at Gopnath where they occur as meter scale pipe like structures with irregular morphology. The pipes have irregular surface morphology and are very friable. They occur at a single level as a mesh of overlapping pipes (Fig. 4a). These are similar to rhizoliths associated with phreatophytic plants, which commonly spread out laterally near the groundwater table from where they source water (Khadkikar et al., 2000).

At one site, bones were observed with the palaeosol (Fig. 4c). This bone bed was concentrated as a

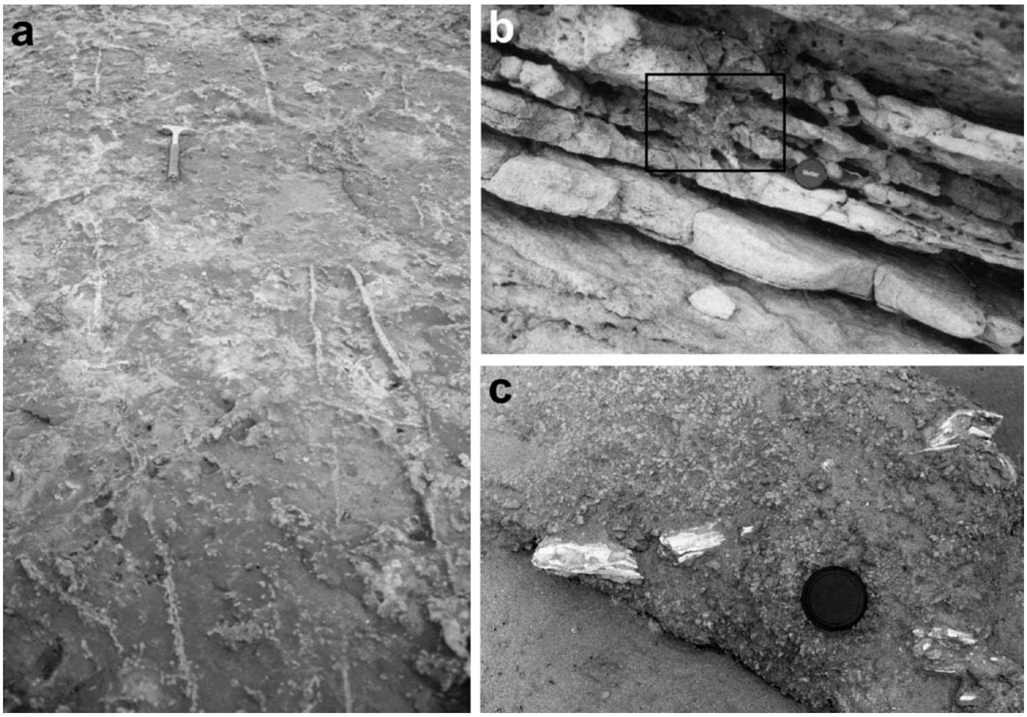

Fig. 4. (a) Rhizoliths occur within the Terra Rossae as root mats. At other places, the mode of occurrence, which is more common, is the presence of near circular planform tubes around which there is a halo of iron oxide formation (b). At a single site near Gopnath, bones were also found associated with the Terra Rossa palaeosols (c).

linear array of white colour fibrous fragments. The bone origin was confirmed in the electron spin resonance spectra, which was obtained for the purpose of dating the palaeosol-forming event. No evidences of human activity in the form of either bones or stone tools were observed. However, Marathe et al. (1998) have reported the presence of stone tools from a Terra Rossa of similar antiquity at Madhuban, which date back to the Lower Palaeolithic.

4.3. Interpretation

The key features of these red beds may be summarized below:

(1) obliteration of sedimentary structures,
(2) down-profile loss in reddening,
(3) clay segregation and platy structure at the top, and presence of blocky aggregates,
(4) sharp upper contact and diffuse lower margin and
(5) presence of residual aeolianite.

These characters suggest that the original aeolianite has been leached away (weathered) to give rise to the red bed. This is confirmed by the general destruction of sedimentary structures, the first observable feature in soil profiles (Retallack, 1990). The presence of blocky aggregates and platy structure manifests ped development, both being common features of the 'A' soil horizons. Also, the down-profile loss in reddening which appears to be due to variations in concentrations of iron oxide is suggestive of pedogenesis. The variable amount of leaching results in different levels of residual carbonate preservation. The soil environment appears to be one that favours strong leaching of carbonate and precipitation of iron oxide. This suggests that the soil was well drained (owing to the absence of gleyed horizons) and experienced oxidizing conditions. Such conditions often come about in seasonal climates (Retallack, 1990). Soil drainage may have been enhanced due to the formation of secondary porosities through karstification (pipe/conduit formation). The formation of spheroidal residual carbonate nodules is enigmatic. It could be possible that this morphology was produced through pedogenesis on a Type 3 karst. In the case of Type 3 karst, the walls are significantly thicker and progressive erosion of the conduits may have led to the formation of this nodular morphology.

Sedimentologists distinguish between red beds of sedimentary and pedogenic origin. Red-coloured soils were classified by Pye (1983) into four principal types. These are Red Latosols, Red Podzols, Red desert soils and Red Mediterranean soils. The latter are termed Terra Rossa when they develop over limestones (Bronger and Bruhn-Lobin, 1997) and are usually seen in the coastal Mediterranean region where they are characterized by a red to brick red colour, which owes its origin to the presence of hematite (Yaalon, 1997). However, the climatic regimes are different from Saurashtra and hence the red beds may best be referred to as Terra Rossa-like soils.

5. Mineralogy and magnetic susceptibility

5.1. Mineralogy

Bulk X-ray diffractometric studies on clays of the palaeosols show a larger dominance by calcite, quartz and some montmorillonite. The iron mineral phase signal is not observed on XRD probably owing to the crypto-crystalline nature of the mineral phase. However, the presence of hematite is observed in Fourier transform infrared spectra taken on the soil samples as a peak at 470 cm^{-1}. This peak is seen associated with the silica peak that occurs at 462 cm^{-1}, which together form a broad hump.

5.2. Magnetic susceptibility

Three Terra Rossa events (Figs. 5 and 6) are observed in the stratigraphic record of which the second event (TR Event 2) is the most ubiquitous. The oldest event (TR Event 1) is observed at two different locations at Gopnath. The second event is also observed at Madhuban from where Marathe et al. (1998) reported Lower Palaeolithic stone tools. The age of the lower Palaeolithic in western India is about ~ 130–100 ka BP (Khadkikar et al., 1999). This suggests that the Terra Rossa Event 2 formed during the last interglacial period. The older event may then correlate with the 170 ka BP event during which the earth entered an interstadial period similar to Isotope

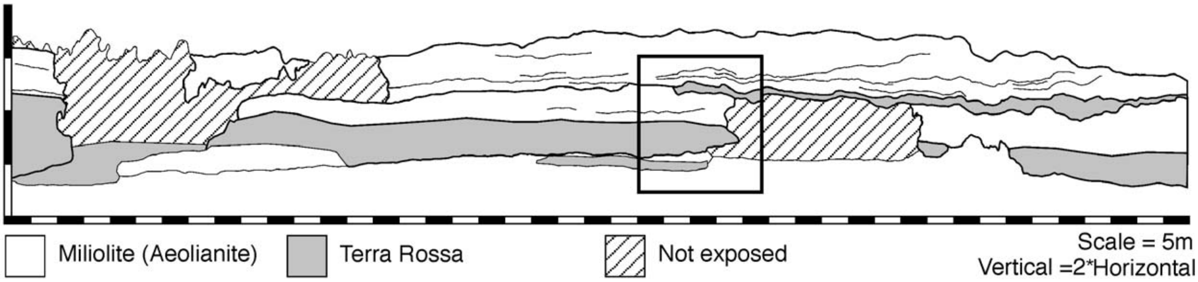

Fig. 5. Overlay of photomosaic at Gopnath showing the principal events of Terra Rossae in southeastern Saurashtra. Of the events shown in the panel Terra Rossa Event 2 is regionally the most extensive and is observed at all the sites from Gopnath to Methla (see Fig. 1 for locations). The highlighted area is further shown in Fig. 6.

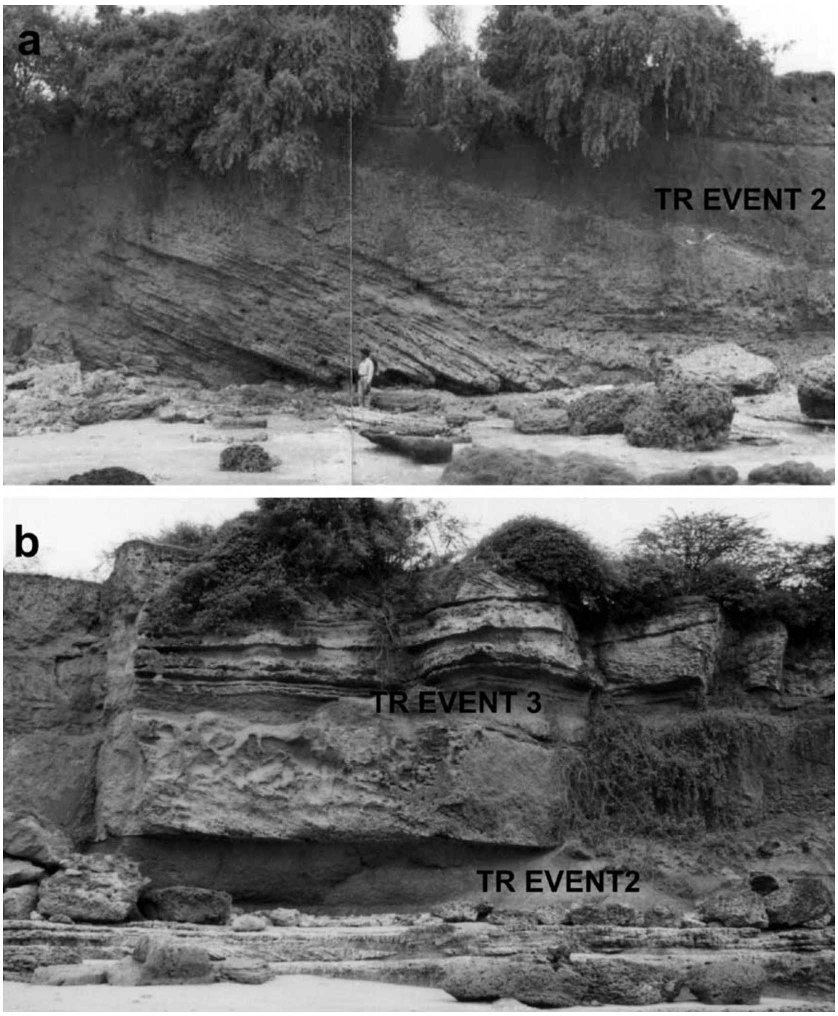

Fig. 6. Terra Rossae inter-stratified with aeolianites at the classic exposure of Gopnath along with their event stratigraphy and notations.

Stage 3. Consequently, it appears that the Terra Rossae have formed during periods of interglacial style of climates that were also durations of increased Southwest Indian Monsoon rainfall.

Mass specific susceptibility (χ) or susceptibility per unit weight of the sample ($\chi = \kappa/\rho$; κ = volume susceptibility and ρ = density) was measured on a Bartington Instruments MS2B Dual Frequency Meter and Sensor (noise level 3×10^{-9} m^3 kg^{-1} for 10-g samples) in magnetic fields of low (0.47 kHz) and high (4.7 kHz) frequencies (χ_{lf} and χ_{hf}). From these data, the coefficient of frequency dependent susceptibility, χ_{fd}=[$100(\chi_{lf} - \chi_{hf})/\chi_{lf}$] was calculated. Anhysteretic remanent magnetization (ARM) grown in a shielded demagnetizer using a peak AF field of 100 mT and a DC field of 0.05 mT was measured on a Minispin fluxgate magnetometer with a noise level of 10^{-7} A m^2 (Molspin, UK). The record of variations in susceptibility (χ) and ARM outlines the changing concentration of magnetic minerals while χ_{fd} provides estimates of the proportion of magnetic minerals of pedogenic origin (Thompson and Oldfield, 1986). A total of 38 hand-specimen samples collected from palaeosols within Late Quaternary aeolianite deposits of southeastern coastal Saurashtra (Fig. 1) were measured for mineral magnetic markers in terms of χ_{lf}, χ_{hf}, χ_{fd} and ARM.

Magnetic susceptibility and frequency dependent susceptibility (χ_{lf} and χ_{fd}) vary from 200 to 1200 (Fig. 7a,b) and from 1% to 2.5%, respectively. However,

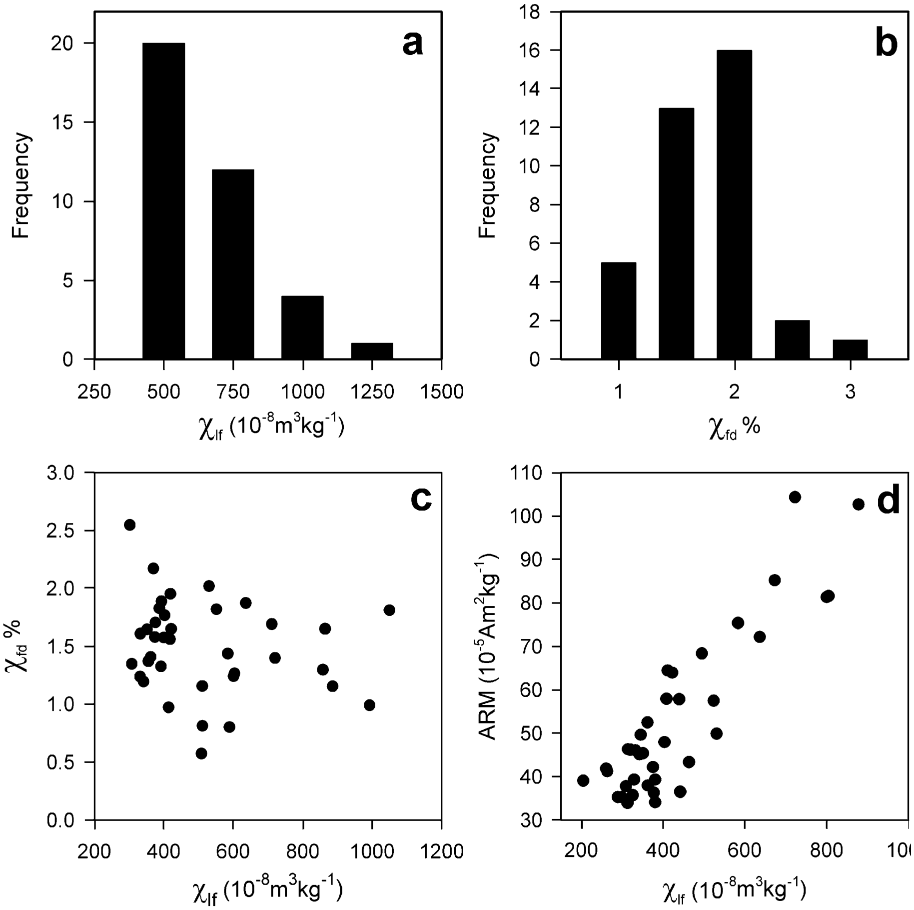

Fig. 7. Histograms showing the frequency distribution of (a, b) low and frequency-dependent susceptibility (χ_{lf} and χ_{fd}). Both these parameters do not covary as shown in (c). (d) Bivariate plot of ARM and magnetic susceptibility χ_{lf}, which shows that they are positively correlated, implying a genetic relationship.

they do not show any covariation (Fig. 7c). On the other hand, ARM shows a good covariation with χ_{lf} (Fig. 7d). This suggests that the primary source of magnetic susceptibility variation in the Terra Rossa profiles is single-domain (SD) magnetite, which is represented by ARM. χ_{fd}, which is a measure of ultrafine superparamagnetic (SP) grains, does not correlate with ARM.

There is little variation between profiles (Figs. 8 and 9) for all the three Terra Rossa events. However, in all profiles, it is worth noting that χ_{lf} and ARM show concurrent changes. But this is not true for χ_{fd} variation, which at times has an inverse relationship with χ_{lf}.

It appears that down-profile changes in magnetic properties are due to the formation of SD magnetite through a breakdown of multi-domain (MD) magnetite particles (detrital, derived from a basaltic provenance). The breakdown during weathering is accompanied by the formation of hematite. Hematite is observed in petrographic studies as a ubiquitous red staining, which is on account of the authigenic iron mineral phase being released during weathering. The ultrafine SP grains may also be a product of this

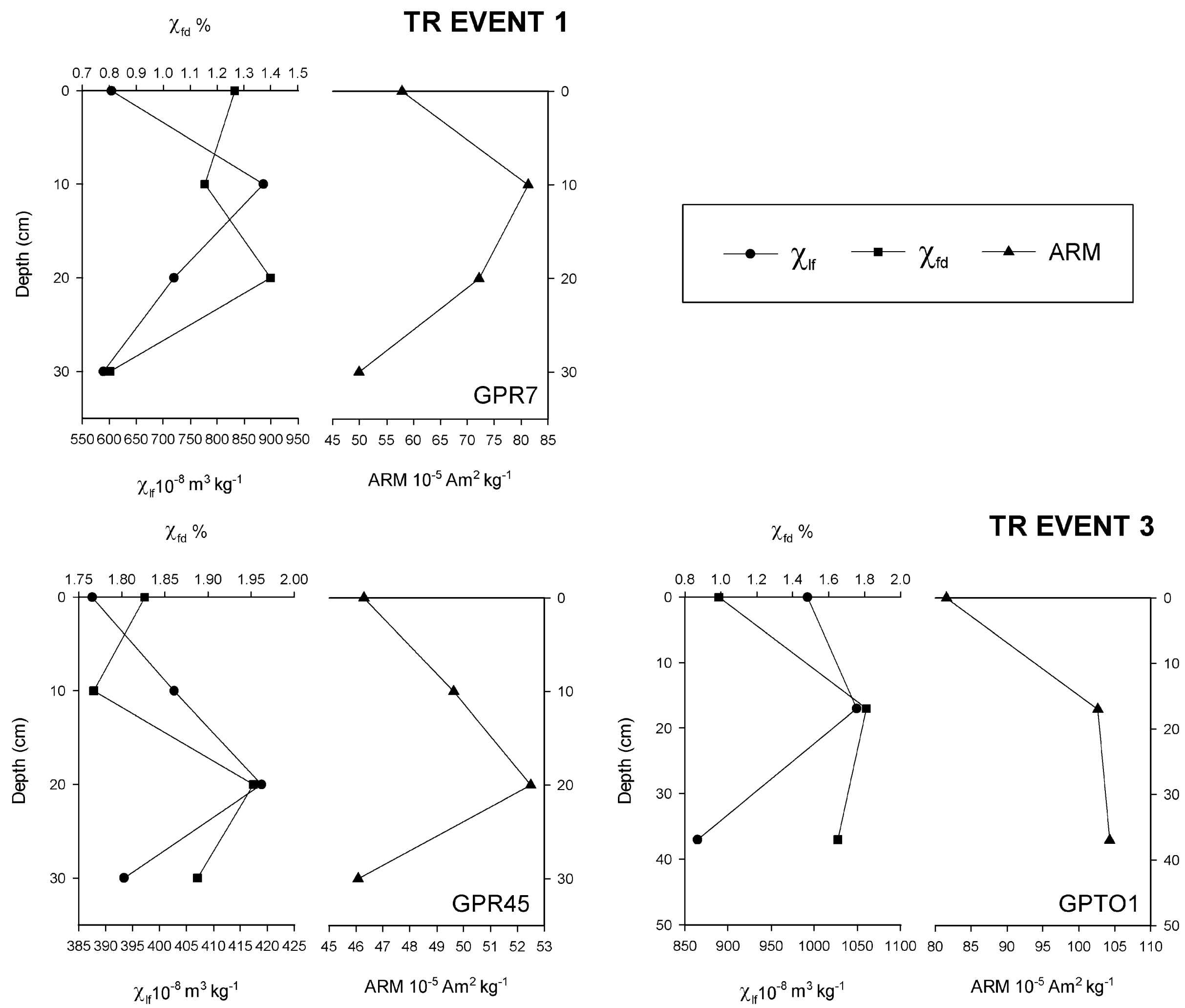

Fig. 8. Summary chart showing magnetic susceptibility and frequency-dependent susceptibility (χ_{lf} and χ_{fd}) along with ARM for Terra Rossae Events 1 and 3. Details are described in the text.

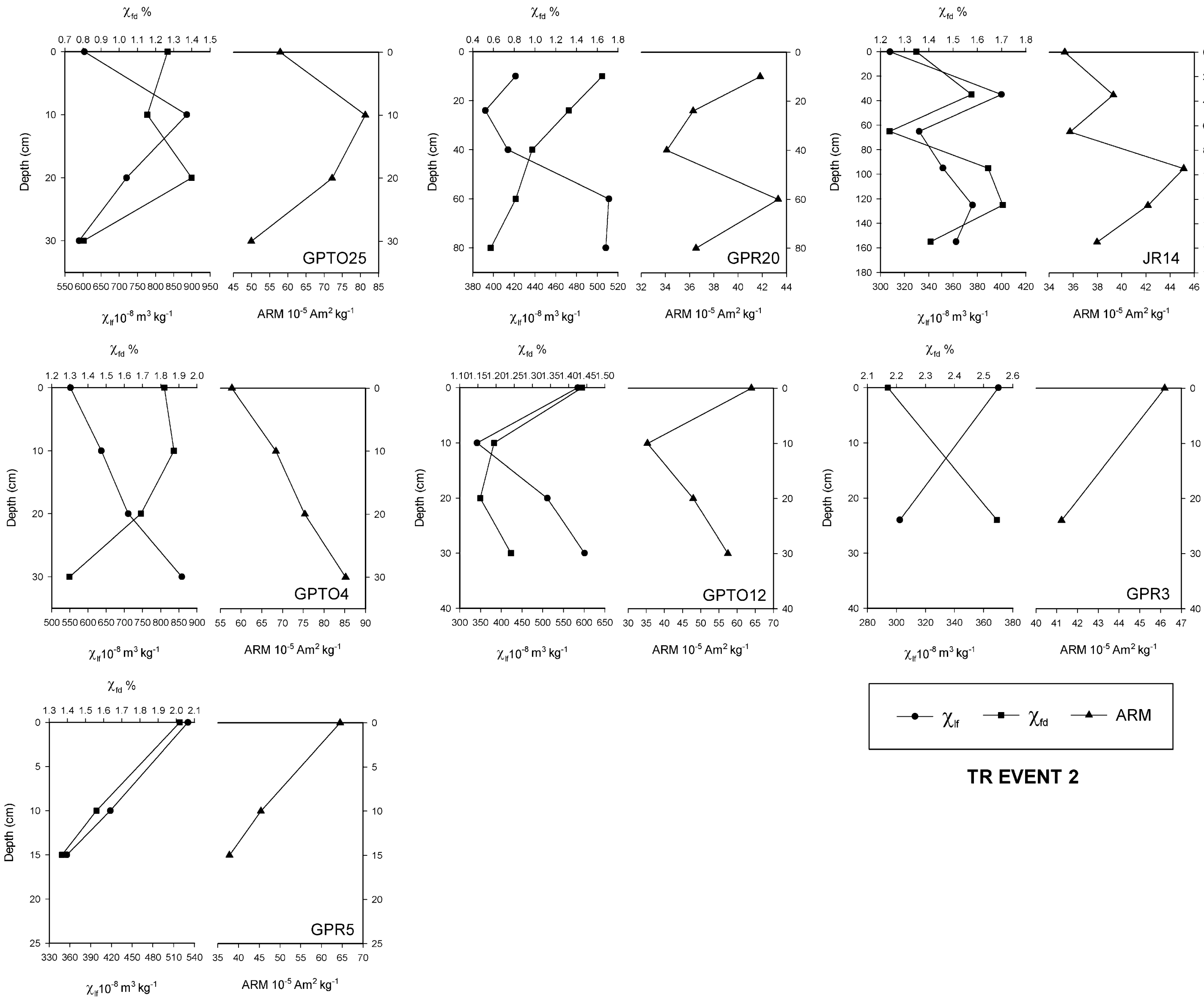

Fig. 9. Summary chart showing magnetic susceptibility and frequency dependent susceptibility (χ_{lf} and χ_{fd}) along with ARM for Terra Rossae Event 2. Details are described in the text.

weathering, but their concentration varies considerably. It may thus be argued that the degree of weathering was not intense enough to produce larger concentrations of ultrafine SP grains but was sufficient for SD grain production. The formation of hematite through this process implies the role of oxidative processes.

Magnetic susceptibility varies down profile and is largely governed by the presence of magnetite and the amount of calcium carbonate. Whereas the former enhances the susceptibility signal, the latter dilutes the magnetic material content leading to lows in the observed magnetic susceptibility profiles. While some profiles such as Gpr20 and Gpto4 showed an inverse relationship between χ_{lf} and χ_{fd}, the majority of the profiles do not show any explicit trend (Fig. 8). This is also brought out when χ_{lf} is plotted against χ_{fd}, which shows a large scatter in the values. Petrographic examination of the Miliolite shows that the diamagnetic and paramagnetic component is represented largely by carbonate, quartz, feldspar and basaltic lithoclasts. The bioclasts are stained red with haematite. It appears that the down-profile changes in the χ_{lf}, χ_{fd} and ARM values are complex and are related to both changes in concentrations of siliciclasts, carbonate, production of haematite—all these contributing to the dilution of the susceptibility signal and the presence of SD and SP magnetic grains, which contribute to increasing the susceptibility.

Several models have been proposed to date to explain the variations in mineral magnetic properties of soils (Dearing et al., 1996; Maher, 1998). These include the effect of forest burning, enhancement of signal due to carbonate leaching and the enhancing effect of organic matter. Recently, the role of microbial magnetite has also been analyzed as a significant contributor to soil susceptibility. Based on an extensive study of British soils, Dearing et al. (1997) demonstrated that the above mechanism does not play a pivotal role in controlling the χ_{fd} of soils. According to them, the accumulation of secondary ferrimagnetic minerals results due to the formation of ferrihydrite as the initial mineral phase under a strong supply of Fe. Bacterial Fe reduction causes ferrihydrite to transform to magnetite, which over time, oxidizes to maghemite. Maher (1998) studied modern and fossil soils from the Chinese loess plateau and showed that magnetite and maghemite are the principal contributors to susceptibility in magnetically enhanced soils. This enhancement is restricted to regions that experience a seasonally wet/dry cycle containing soils that are well drained and have a primary source for iron. In case of the Miliolite Terra Rossae, the formation of secondary ferrimagnetic minerals appears to have been governed by the monsoonal climate. During seasonal wetting in the monsoon months, breakdown of MD magnetic grains would have been facilitated leading to the formation of SD and SP magnetic grains; the formation of hematite restricted during the dry hot summers through oxidation of the magnetite. Local variations in χ_{lf} profiles also appear to be governed by the relative abundance of canted antiferromagnetic iron oxides like haematite and diamagnetic minerals such as clays, carbonate and quartz. This seems to contradict the observation that ultrafine SP magnetite particles contribute 90% of the susceptibility signal in Chinese Loess (Maher and Thompson, 1992). Our observation casts some doubt on the general validity of mainly pedogenically ultrafine magnetic production, at least for the studied Terra Rossae profiles. It supports the conclusion of Meng et al. (1997) that the origin of magnetic susceptibility signal is still rather poorly understood.

6. Discussion

Looking at the entire gamut of karst and palaeosol types, it is possible to think of them as part of an evolutionary or palaeontologically speaking ontogenetic (growth) sequence. Several factors affect soil formation (Retallack, 1990). Of these, key parameters that appear to play a major role in the present case appear to be climate, topography and duration of weathering. However, the factor of topography (catenal effect) may be isolated by examining the same topographic levels (or palaeotopographic levels). These can be readily identified by noting the nature of the upper bounding surface (slope), which is horizontal in regions of maximum soil development. The remaining factors govern the soil formation/karst formation. A given aeolianite suffers diagenesis the moment meteoric water interacts with it, leading to early cementation and hardening. Through repeated rainfall events in which meteoric water fluxes increase through the soil, carbonate dissolution begins at inter-granular spaces leading to the formation of Type 1 karst. This forms Stage 1 of the ontogenetic sequence (Fig. 10). The chaotic distribution and orientation of cavities gives its characteristic spongy appearance.

Successive waters have a larger through flow due to the generation of secondary porosity due to the formation of Type 1 karst. This enhances gravity flow and vertical conduit formation takes place. The exact reason for this is unclear but is probably related to concentration of meteoric waters at certain nuclei, i.e., common intersections/junctions in the network of Type 1 karst. Such network junctions may provide sites of cavity formation, which progressively extend downwards through time. The formation of vertical conduits is the distinctive character of Type 2 karst, and, together, the occurrence of Type 1 and 2 karst identifies the second stage in the ontogenetic sequence (Fig. 10). This has also been demonstrated through modelling of karst systems (Palmer, 1998; Annable and Sudicky, 1998), which shows that during initial interaction of groundwater with limestone, all fissures enlarge simultaneously at the same rate that progressively enlarge down profile.

Similarly, the accumulation of water from vertical conduits creates large channel networks deeper in the profile. The principal factor appears to be the attainment of a certain critical volume of meteoric water, which permits the formation of channels with large diameters/cross sectional areas. Support for this interpretation comes from the fact that such larger channels/conduits occur always deeper in the profile and never are seen at shallower levels. This forms Stage 3 (Fig. 10).

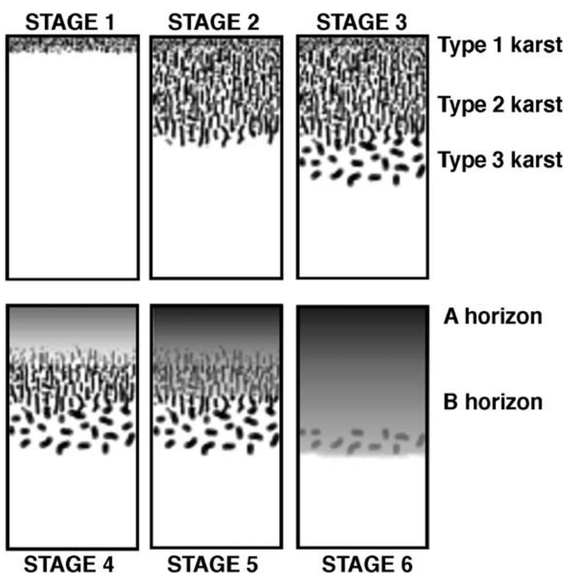

Fig. 10. Ontogenetic model for epikarst and palaeosol development in the aeolianites of Saurashtra.

Progressive weathering of the aeolianite after this stage begins with weathering of the silicate minerals as well in a large way. The weathering of ferromagnesian minerals leads to clay neoformation and sesquioxide formation. Also, the breakage of the sediment fabric takes place as silicates are attacked by the meteoric waters causes obliteration of the primary lamination. This initial stage of reddening marks the beginning of Stage 4 (Fig. 10). The degree of pedogenesis increases to form deeper hues of reddening and residual aeolianites in Stage 5 (Fig. 10). Complete disappearance of residual aeolianite and significant clay mineral accumulation at the top of the profiles takes place during Stage 6. Both Stage 5 and Stage 6 soils are characterized by horizonation and the development of a horizontal platy-like fabric at the top (A horizon).

The evolutionary sequence thus may represent two features in the soil-weathering environment. One is different durations of exposure and the other an incremental rise in recharge and net meteoric water flux. The latter appears to be more logical as the formation of Stage 3 requires larger throughflow of meteoric water and may not be attained due to simple rise in exposure time to the atmosphere hydrosphere and biosphere.

This is particularly well reflected in the six-stage model of karst and Terra Rossa soil formation. Its ontogenetic nature suggests that for Stage 6 soils to form, it went through all the previous stages. These stages reflect an increment in the available water budget (~ rainfall). Consequently, the presence of Terra Rossa type soils reflects a progressive increase towards higher mean annual rainfalls comparable to the modern values near 600–700 mm. These soils mark the transition from a stadial/glacial period to an interstadial/interglacial period. The presence of three such Terra Rossa palaeosols suggests that these apparently correspond to the Marine Isotope Stages 3, 5 and 7. Relative smaller ameliorations in the intensity (rainfall) of the Indian Summer Monsoon led to karstification of the Stages 1–3 types.

7. Conclusion

Late Quaternary aeolianites of the southeastern coast of Saurashtra in western India show a wide array of epikarst and red-soil formation, and serve to typify the character of aeolianite weathering under a monsoonal climate. Three varieties of epikarst are identified that represent down-profile increase in groundwater flow. Five types of Terra Rossae represent a transition from the karstified limestone to soil development. Terra Rossae differ in the content of residual aeolianite and show both simple and complex profiles. The latter at places shows ped development. The results show that an ontogenetic (growth) sequence exists from incipient epikarst to complex palaeosols. This ontogenetic sequence represents an incremental increase in the groundwater budget of the region in response to changing intensification of the Indian monsoon rainfall.

The magnetic susceptibility of Terra Rossae is governed by the concentration of pedogenically produced single-domain and ultrafine superparamagnetic grains and haematite. All the profiles have similar values of the magnetic parameters measured. The down-profile changes in susceptibility are linked genetically to the concentration of single-domain magnetite. It is proposed that weathering of the aeolianite during Terra Rossa genesis leads to breakdown of multi-domain detrital magnetite and formation of both single-domain and superparamagnetic grains and is accompanied by the formation of hematite.

Acknowledgements

The authors thank *Geomorphology* reviewers, Drs. K. White, J. Hannam and Editor Dr. A.M. Harvey, for their critical comments on the manuscript. Financial assistance to ASK vide DST projects is gratefully acknowledged. Dr. T.K. Gundurao (IIT-Bombay, Powai) is thanked for FTIR analyses.

References

Annable, W.K., Sudicky, E.A., 1998. Simulation of karst genesis: hydrodynamic and geochemical rock–water interactions. Bull. Hydrogeol. 16, 211–222.

Bronger, A., Bruhn-Lobin, N., 1997. Paleopedology of Terrae rossae-Rhodoxeralfs from Quaternary calcarenites in NW Morocco. Catena 28, 279–295.

Carter, H.J., 1849. On foraminifera, their organisation and their existence of fossilised state in Arabia, Sindh, Kuth and Kathiawar. J. R. Asiat. Soc. Bombay 3, 153–173.

Das, P.K., 1995. The Monsoons. National Book Trust, India. 252 pp.

Dearing, J.A., Hay, K.L., Baban, S.M.J., Huddleston, A.S., Wellington, E.M.H., Loveland, P.J., 1996. Magnetic susceptibility of soil: an evaluation of conflicting theories using a national dataset. Geophys. J. Int. 127, 728–734.

Dearing, J.A., Bird, P.M., Dann, R.J.L., Benjamin, S.F., 1997. Secondary ferromagnetic minerals in Welsh soils: a comparison of mineral magnetic detection methods and implications for mineral formation. Geophys. J. Int. 130, 727–736.

Herwitz, S.R., Muhs, D.R., Prospero, J.M., Mahan, S., Vaughn, B., 1996. Origin of Bermuda's clay-rich Quaternary palaeosols and their palaeoclimatic significance. J. Geophys. Res. 101D18, 23389–23400.

Jennings, J.N., 1985. Karst. The MIT Press, Massachusetts.

Khadkikar, A.S., Mathew, G., Malik, J.N., Gundu Rao, T.K., Chowgaonkar, M., Merh, S.S., 1999. The influence of the southwest Indian monsoon on late Quaternary continental sedimentation, western India over the past 130 kyrs. Terra Nova 11, 273–277.

Khadkikar, A.S., Chamyal, L.S., Ramesh, R., 2000. The character and genesis of calcretes in late Quaternary alluvial deposits, western India and its bearing on the interpretation of ancient climates. Palaeogeogr. Palaeoclimatol. Palaeoecol. 142, 239–262.

Kindler, P., Hearty, P.J., 1997. Geology of the Bahamas: architecture of Bahamian islands. In: Vacher, H.L., Quinn, T. (Eds.), Geology and Hydrogeology of Carbonate Islands. Developments in Sedimentology, vol. 54. Elsevier Science, Amsterdam, pp. 141–160.

Maher, B., 1998. Magnetic properties of modern soils and Quaternary loessic paleosols: paleoclimatic implications. Palaeogeogr. Palaeoclimatol. Palaeoecol. 137, 25–54.

Maher, B.A., Thompson, R., 1992. Palaeoclimate significance of the mineral magnetic record of Chinese loess and paleosols. Quat. Res. 37, 155–170.

Marathe, A.R., Rajaguru, S.N., Deodhar, P.G., 1998. Coastal miliolite formation and history of early man in southern Saurashtra, western India. In: Alsharhan, A.S., Glennie, K.W., Whittle, G.L., Kendall, C.G.St.C. (Eds.), Quaternary Deserts and Climatic Change. Balkema, Rotterdam, pp. 601–607.

Meng, X., Derbyshire, E., Kemp, R.A., 1997. Origin of magnetic susceptibility signal in Loess. Quat. Sci. Rev. 16, 833–839.

Merh, S.S., 1980. The miliolite problem. Presidential Address 67th Indian Science Congress Proceedings 67, 15–42.

Mylorie, J.E., Carew, J.L., 1995. Karst development on carbonate islands. In: Budd, D., Harris, P.M., Saller, A. (Eds.), Unconformities and Porosity in Carbonate Strata. AAPG Memoir, vol. 63, pp. 55–76. Tulsa.

Palmer, A.N., 1998. Modelling the evolution and morphology of limestone caves. Bull. Hydrogeol. 16, 157–166.

Pye, K., 1983. Red beds. In: Goudie, A.S., Pye, K. (Eds.),

Chemical Sediments and Geomorphology. Acad. Press, London, pp. 227–263.
Retallack, G.J., 1990. Soils of the Past. Unwin Hyman, London.
Thompson, R., Oldfield, R., 1986. Environmental Magnetism. Allen and Unwin, London.
Vacher, H.L., Rowe, M.P., 1997. Geology and hydrogeology of Bermuda. In: Vacher, H.L., Quinn, T. (Eds.), Geology and Hydrogeology of Carbonate Islands. Developments in Sedimentology, vol. 54. Elsevier Science, Amsterdam, pp. 35–90.
Yaalon, D.H., 1997. Soils in the Mediterranean region: what makes them different? Catena 28, 157–169.